Multifunctional fluorophores for live-cell imaging and affinity capture of proteins

Pratik Kumar[1], Jason D. Vevea[2,3], Edwin R. Chapman[2,3], and Luke D. Lavis[1,*]

[1] Janelia Research Campus, Howard Hughes Medical Institute, Ashburn, VA, USA

[2] Department of Neuroscience, University of Wisconsin–Madison, Madison, WI, USA

[3] Howard Hughes Medical Institute, University of Wisconsin–Madison, Madison, WI, USA

*To whom correspondence should be addressed: lavisl@janelia.hhmi.org

ABSTRACT: The development of enzyme-based self-labeling tags allow the labeling of proteins in living cells with synthetic small-molecules. Use of a fluorophore-containing ligand enables the visualization of protein location inside cells using fluorescence microscopy. Alternatively, deployment of a biotin-containing ligand allows purification of tagged protein using affinity resins. Despite these various applications of self-labeling tags, most ligands serve a single purpose. Here, we describe self-labeling tag ligands that allow both visualization and subsequent capture of a protein. A key design principle is exploiting the chemical properties and size of a rhodamine fluorophore to optimize cell-permeability of the ligand and the capture efficiency of the biotin conjugate. This work generates useful "multifunctional" fluorophores with generalizable design principles that will allow the construction of new tools for biology.

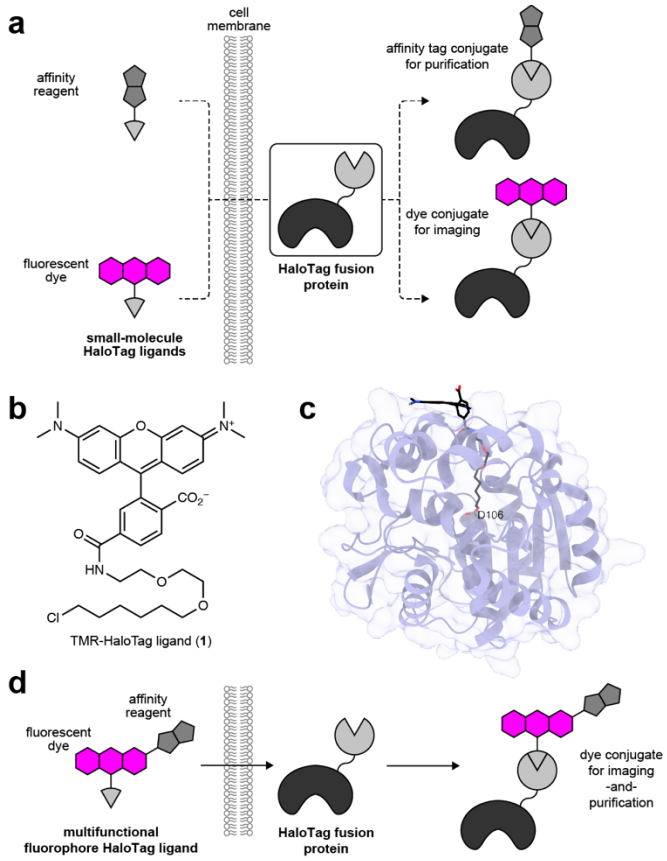

Figure 1. Multifunctional fluorophores to enable both live-cell fluorescence imaging and affinity purification of specific intracellular proteins. (**a**) Current reagents for labeling specific proteins using self-labeling tags typically allow a single application. (**b**) Chemical structure of tetramethylrhodamine-HaloTag ligand used for directed evolution of HaloTag. (**c**) Crystal structure of TMR-HaloTag ligand covalently bound to HaloTag depicting the tight association of HaloTag protein with the covalently linked small-molecule ligand. (**d**) Schematic of multifunctional fluorophores that enable both live-cell fluorescence microscopy and affinity purification of specific intracellular proteins.

INTRODUCTION

Advances in the understanding of biological processes rely on the ability to visualize and manipulate biomolecules inside cells. Research at the interface of synthetic organic chemistry and protein biochemistry has generated powerful tools to probe and perturb cells with molecular specificity[1]. In particular, the engineering of enzyme–substrate interactions produced self-labeling tags such as the HaloTag[2] or SNAP-tag[3]. These protein tags react specifically and irreversibly with a ligand motif that can be appended with a variety of functionalities including affinity tags for purification and fluorescent dyes for visualization (**Figure 1a**)[4]. In addition to intracellular labeling

experiments, self-labeling tags can also serve as a robust scaffold for indicators[5, 6] and integrators[7] of cellular activity.

Despite the generality of self-labeling tags, the current portfolio of ligands suffers from limitations. Most ligands serve a single function—for example to probe or purify the tagged protein. Second, each combination of functional small-molecule, linker, and ligand moiety has distinct chemical properties that can affect the cell permeability and labeling kinetics of the ligand, and the properties of the resulting protein conjugate[8]. For the development of the HaloTag system, the directed evolution approach utilized a 1-chlorohexane ligand attached to a 6-carboxytetramethylrhodamine (TMR) via a short polyethylene glycol (PEG) linker[2]. This TMR-HaloTag ligand (**1**, **Figure 1b**) is cell-permeable, exhibits rapid labeling kinetics with the HaloTag, and results in a close association of the TMR moiety and the surface of the protein (**Figure 1c**; PDB: 6U32). This intimate dye–protein contact can elicit modest improvements in fluorophore photophysics, but for other moieties this close association of protein and ligand can be detrimental, requiring the incorporation of longer linkers that can affect cell-permeability and other ligand properties.

Given the common tug-of-war between functionality and biocompatibility in small-molecule ligand development, we envisioned a new strategy to create cell-permeable probes by utilizing a rhodamine fluorophore as a linker for self-labeling tag ligands (**Figure 1d**). This idea was predicated on several factors. First, as mentioned above, the directed evolution of the HaloTag utilized TMR-based ligand **1**, and rhodamine-based HaloTag ligands generally show rapid labeling kinetics[8]. Second, the ability to fine-tune the chemical and spectral properties of rhodamine dyes could allow optimization of the cell-permeability or other properties of the ligand[9-12]. Finally, the insertion of a fluorescent species enables visualization of the molecule inside cells, allowing

verification of the compound's performance using fluorescence imaging. Here, we describe our design and optimization of fluorophore ligands bearing a biotin that is both cell-permeable and useful for subsequent purification of HaloTag fusion proteins. These modular "multifunctional fluorophores" represent a new facet of dye-based tools for biology and this strategy should be generalizable to other functional motifs.

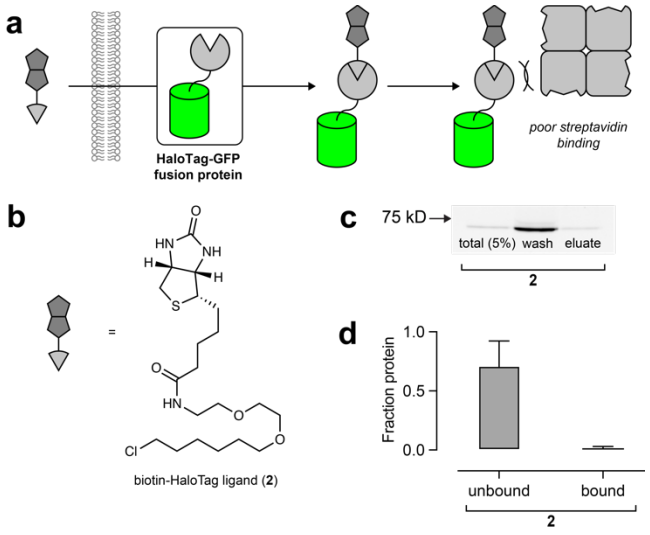

Figure 2. Performance of biotin-HaloTag ligand (2). (**a**) Schematic of assay to evaluate performance of biotin-HaloTag conjugates. (**b**) Chemical structure of commercially available biotin-HaloTag ligand (**2**). (**c, d**) SDS-PAGE/in-gel fluorescence (**c**) and quantification (**d**) showing the amount of msGFP fusion protein bound to streptavidin using ligand **2**.

RESULTS AND DISCUSSION

Evaluation of biotin-HaloTag ligand. We first evaluated HaloTag ligands bearing biotin given the broad utility of the high-affinity biotin–streptavidin interaction in biochemistry and cell biology. To test these compounds, we developed an assay where the HaloTag is expressed as a fusion with monomeric superfolder green fluorescent protein (msGFP); the construct also included an OMP25 sequence to localize the fusion protein to the outer mitochondrial membrane allowing straightforward imaging and protein capture experiments[13, 14]. Cells expressing this fusion protein were incubated with biotin-containing HaloTag ligands followed by washing and cell lysis. The

crude supernatant was incubated with streptavidin-coated magnetic microbeads, applied to a column and the elution fractions were analyzed by SDS–PAGE and in-gel fluorescence (**Figure 2a**). We first tested the commercial biotin-HaloTag ligand (**2**, **Figure 2b**), which has the standard HaloTag ligand found in compound **1** (**Figure 1b**) directly attached to the biotin carboxyl group. Pulse–chase experiments revealed compound **2** is modestly membrane permeable and can label the HaloTag–msGFP fusion in living cells when applied at μM concentrations (**Supplementary Figure 1**). The standard PEG_2 linker in compound **2** is too short to allow binding of the biotin–HaloTag conjugate to streptavidin, however, which prevents purification of HaloTag fusion proteins from cells using streptavidin (**Figure 2c–d**). Unfortunately, attempts to remedy this problem by incorporating a longer PEG linker yields a molecule with no detectable cell permeability, thereby rendering it unsuitable for live-cell experiments[15].

Design and synthesis of biotin-containing multifunctional fluorophores. We posited the problems with the extant biotin-containing HaloTag ligands could be remedied by incorporating a rhodamine linker into the chemical structure. For base rhodamine dyes, we envisaged utilizing the Janelia Fluor (JF) dyes JF_{549} (**3**), JF_{646}, (**4**), and JF_{635} (**5**, **Figure 3a**). JF_{549} (**3**) is structurally similar to TMR, but contains four-membered azetidine rings in place of the *N,N*-dimethylamino groups; this net increase of two carbon atoms greatly increases brightness and photostability[16]. JF_{646} (**4**) is a Si-rhodamine where the xanthene oxygen in **3** is replaced with a dimethylsilicon group[17, 18]. This substitution elicits a substantial ~100 nm bathochromic shift in absorption maxima (λ_{abs}) and fluorescence emission maxima (λ_{em}). JF_{635} (**5**) contains 3-fluoroazetidine substituents that fine-tune the properties of the Si-rhodamine molecule, eliciting a modest 11-nm hypsochromic shift in both λ_{abs} and λ_{em}[9].

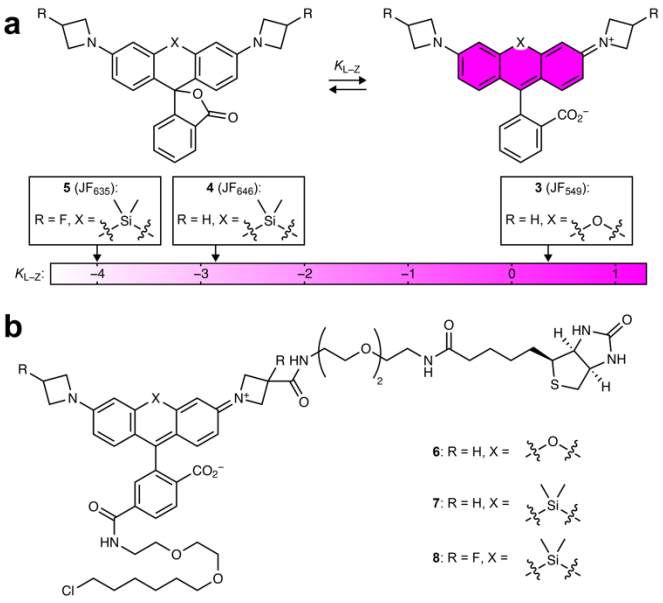

Figure 3. Design of biotin-JF-HaloTag ligands. (**a**) Schematic showing the dynamic equilibrium between the nonfluorescent lactone (L) forms and fluorescent zwitterionic (Z) forms along with the lactone–zwitterion equilibrium constant ($K_{L–Z}$) for rhodamine-based Janelia Fluor (JF) dyes **3**–**5**. (**b**) Chemical structures of biotin-JF-HaloTag ligands **6**–**8**.

A key property of rhodamine dyes is an equilibrium between a nonfluorescent lactone (L) and fluorescent zwitterion (Z; **Figure 3a**). This equilibrium dictates the performance of dyes in biological systems. In previous work, we developed a general rubric linking the lactone–zwitterion equilibrium constant ($K_{L–Z}$) of the JF dyes with properties such as cell permeability and fluorogenicity[19]. In addition to modulating spectral characteristics, chemical substitutions can also affect $K_{L–Z}$. JF_{549} (**3**) has a relatively high $K_{L–Z}$ = 3.45 so it preferentially adopts the zwitterionic form. The dimethylsilicon substitution in JF_{646} (**4**) causes a large shift in equilibrium toward the nonfluorescent lactone form ($K_{L–Z}$ = 0.0014). The electron-withdrawing fluorines in JF_{635} (**5**) further shift this equilibrium ($K_{L–Z}$ = 0.0001), yielding a dye with low visible absorption even in polar media such as water. Together, this series of dyes represent different foundational chemical properties to test if rhodamine moieties could be used to improve cell permeability.

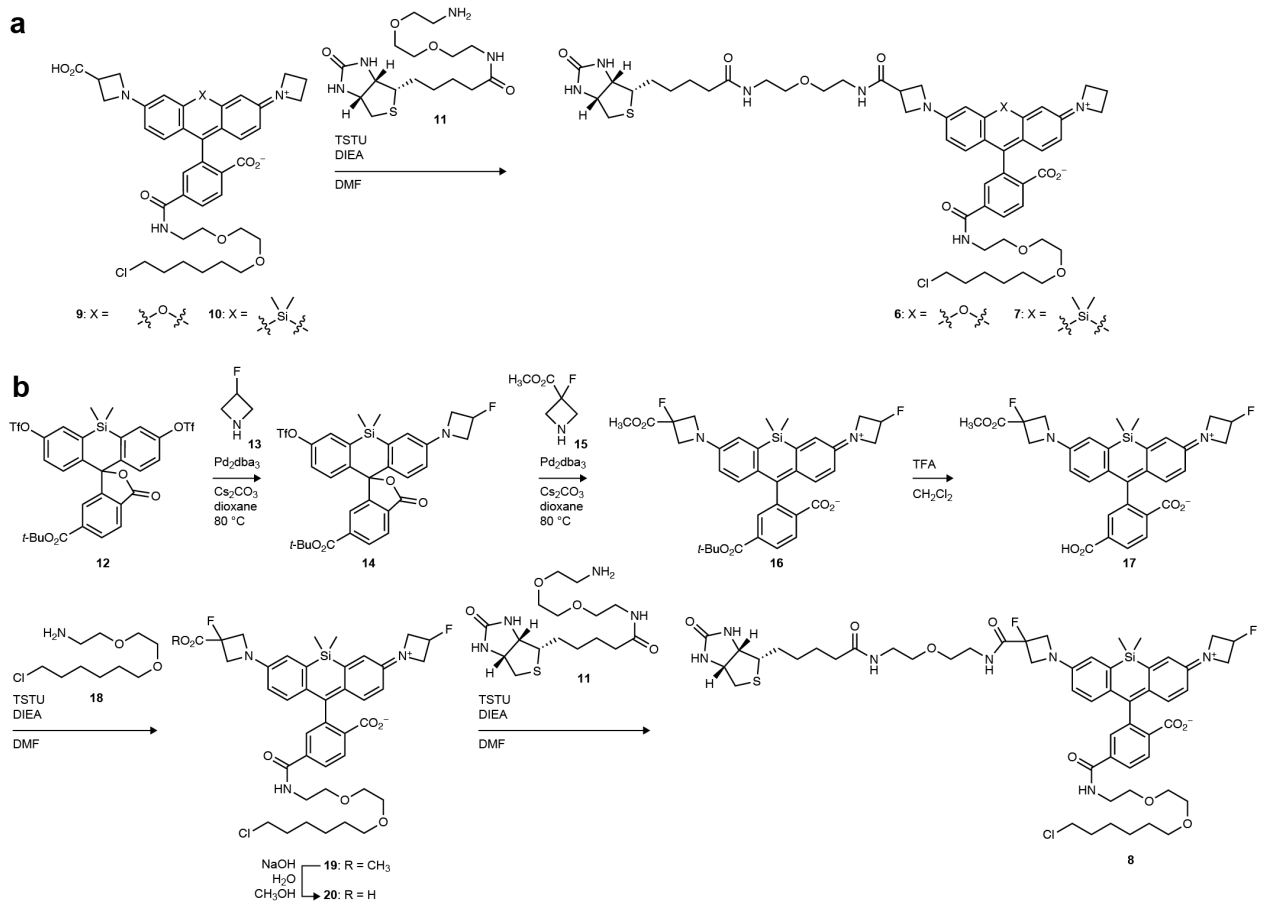

Scheme 1. Synthesis of biotin-JF-HaloTag ligands.

We then considered the installation of the biotin group. In addition to improving brightness and allowing fine-tuning of spectral properties and K_{L-Z} (*e.g.*, JF_{635}, **5**), the azetidine motif also allows facile conjugation of chemical groups using 3-carboxyazetidine derivatives. In previous work, we attached the Ca^{2+} chelator BAPTA to prepare localizable calcium ion indicators[5]. Using this strategy, we synthesized the biotin-JF-HaloTag ligand compounds **6**–**8** (**Figure 3b**). The biotin-JF_{549}-HaloTag ligand (**6**) and biotin-JF_{646}-HaloTag ligand (**7**) were prepared by conjugating the known 3-carboxyazetidine compounds **9** and **10** with the commercially available biotin-PEG_2-NH_2 (**11**; **Scheme 1a**). The JF_{635} derivative **8** was synthesized starting from the Si-fluorescein ditriflate derivative **12** (**Scheme 1b**). Sequential palladium-catalyzed C–N cross-coupling

reactions first with 3-fluoroazetidine (**13**) to generate **14**, followed by 3-carboxyazetidine methyl ester (**15**) generated Si-rhodamine **16** in 55% yield over two steps. Subsequent deprotection of the *t*-butyl ester by trifluoroacetic acid (TFA) generated the carboxy-containing dye **17**, which was coupled to the standard HaloTag ligand amine **18** to yield compound **19**. This was followed by mild saponification of the methyl ester to afford compound **20** in 61% yield over three steps. Finally, amide coupling of **20** and biotin-PEG_2-NH_2 (**11**) afforded biotin-JF_{635}-HaloTag ligand (**8**) in 28% yield.

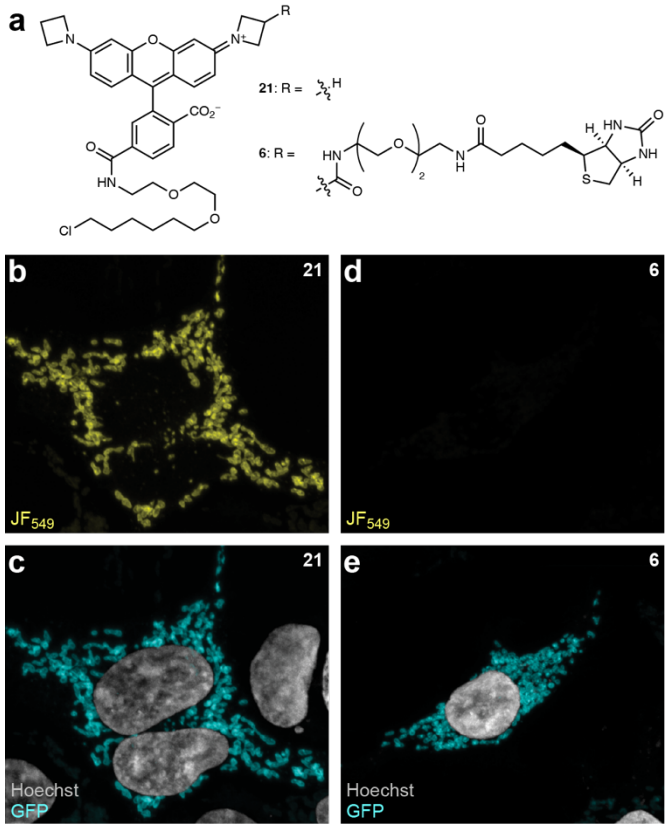

Figure 4. Evaluation of biotin-JF_{549}-HaloTag ligand (6). (**a**) Chemical structures of the JF_{549}-HaloTag ligand (**21**) and biotin-JF_{549}-HaloTag ligand (**6**). (**b**–**e**) Fluorescence microscopy images of live HEK293T cells expressing msGFP-HaloTag fusion localized to the mitochondrial outer membrane after incubation with either JF_{549}-HaloTag ligand (**21**; **b**,**c**) or biotin-JF_{549}-HaloTag ligand (**6**; **d**,**e**) and counterstained with Hoechst 33342.

Cellular experiments with biotin-containing ligands. We then tested the biotin conjugates in cellular experiments, starting with the biotin-JF_{549}-HaloTag ligand (**6**), comparing this to the

standard HaloTag ligand of JF_{549} (**21**, **Figure 4a**). Although the parent compound **21** labeled the mitochondria-localized HaloTag-msGFP fusions inside cells (**Figure 4b–c**), the biotin-containing ligand **6** did not show appreciable cellular labeling measured using fluorescence microscopy (**Figure 4d–e**, **Supplementary Figure 2**). This result demonstrates that the proclivity of JF_{549} to adopt the polar zwitterionic form ($K_{L–Z}$ = 3.5, **Figure 3a**) combined with the hydrophilic biotin–PEG functionality yields a molecule that exhibits low membrane permeability in cellular experiments.

We then tested the biotin-JF_{646}-HaloTag ligand (**7**) and parent JF_{646}-HaloTag ligand (**22**; **Figure 5a**). As expected, fluorescence microscopy experiments revealed that the established JF_{646} ligand **22** labeled the HaloTag-msGFP fusion protein inside cells (**Figure 5b–c**). In contrast to the JF_{549} compound **6** (**Figure 4d–e**), however, the biotin-containing JF_{646} ligand **7** also labeled proteins inside cells at nM concentration (**Figure 5d–e**); incubation of live cells with the ligand gave almost immediate far-red cellular fluorescence. The biotin-JF_{635}-HaloTag ligand (**8**) and the unsubstituted JF_{635}-HaloTag ligand (**23**; **Figure 5f**) gave different results. Relatively bright labeling of mitochondria was observed with the parent ligand **23** (**Figure 5g–h**), but the signal from cells incubated with biotin-JF_{635} ligand **8** was lower (**Figure 5i–j**). The imaging experiments using biotin-JF-HaloTag ligands **7**–**8** and JF-HaloTag ligands **22**–**23** were repeated and quantified (**Figure 5k**), showing that the two JF_{646} ligands exhibit similar average intensities. For the JF_{635} derived compounds, the biotinylated **8** showed lower fluorescence intensity than the unmodified ligand **23**; both JF_{635} compounds exhibited lower intensity than the JF_{646} compounds.

We then tested the efficiency of labeling by cell lysis and capture of biotin-labeled protein using streptavidin beads (**Figure 5l**). As expected, the use of the non-biotinylated JF_{635}-HaloTag ligand (**23**) gave no appreciable protein capture. Use of the biotin-JF_{635}-HaloTag ligand (**8**), however,

showed efficient labeling of protein, yielding a capture efficiency of 45%; this was equivalent to the capture efficiency of the biotin-JF_{646}-HaloTag ligand (**7; Figure 5l–m**).

This result was inconsistent with the different fluorescence intensities observed in cells using the two biotin ligands (**Figure 5d, 5i**). To resolve this discrepancy, we measured the absorbance of **7** and **8** in the absence (−HT) or presence (+HT) of excess purified HaloTag protein (**Figure 5n**). For the JF_{646} ligand **7**, we observed relatively high absorptivity in the unbound state; attachment to the HaloTag protein increased the absorption two-fold. For the JF_{635} compound **8**, the free ligand showed relatively low absorption in solution and showed a substantial, 10-fold increase upon conjugation to the HaloTag protein but with an overall lower absorbance compared to JF_{646} ligand **7**. These results show that the JF_{635} ligand **8** is highly chromogenic and fluorogenic, but has lower absolute absorptivity compared to the JF_{646} ligand **7** in the HaloTag-bound state, leading to lower fluorescence intensity in cells. Overall, this demonstrates that both Si-rhodamine-based biotin-JF-HaloTag ligands **7** and **8** enter cells, efficiently label HaloTag proteins, and present a biotin moiety that is accessible to streptavidin affinity resins for protein capture.

CONCLUSION

The ability to specifically label proteins with synthetic small-molecules inside living cells is a powerful technique for biology. In particular, the development of fluorescent ligands for self-labeling tags has enabled advanced imaging experiments. Most synthetic ligands only serve a single purpose, however, and many compounds suffer from poor cell-permeability. We addressed these issues through the rational design of multifunctional dyes that contain both a rhodamine fluorophore and a biotin affinity reagent. A critical element in our molecular design was to exploit the different chemical properties of rhodamine dyes to give functional biotin derivatives with high

cell permeability. Looking forward, this strategy of "rhodamine-as-linker" should permit the creation of superior tools for cell biology, allowing a single compound to serve as both a fluorescent label and protein manipulator.

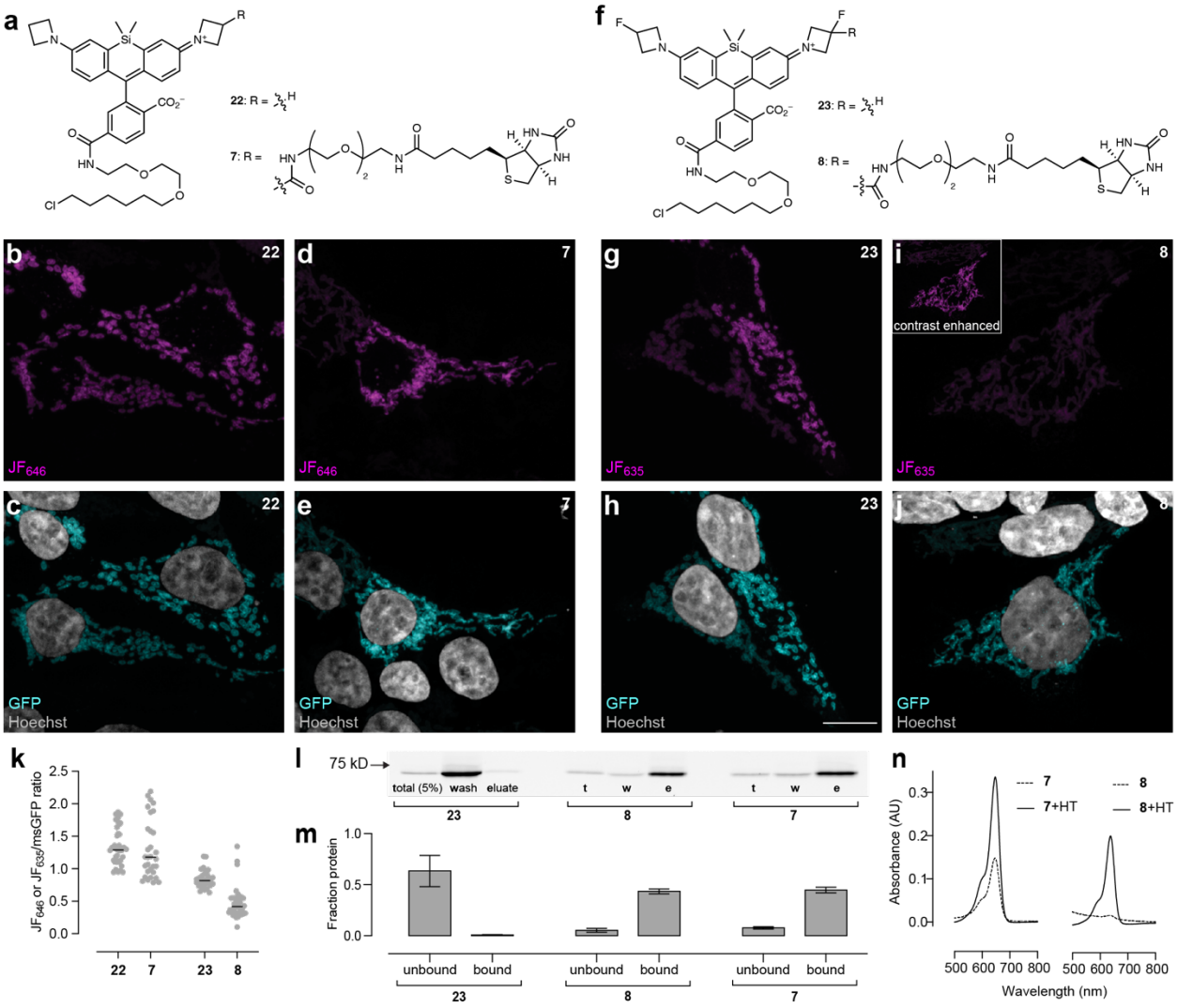

Figure 5. Evaluation of biotin-JF$_{646}$-HaloTag ligand (7) and biotin-JF$_{635}$-HaloTag ligand (8). (**a**) Chemical structures of **7** and parent ligand JF$_{646}$-HaloTag ligand (**22**). (**b**–**e**) Fluorescence microscopy images of live HEK293T cells expressing msGFP-HaloTag fusion localized to the mitochondrial outer membrane after incubation with either JF$_{646}$-HaloTag ligand (**22**; **b**,**c**) or biotin-JF$_{646}$-HaloTag ligand (**7**; **d**,**e**) and counterstained with Hoechst 33342. (**f**) Chemical structures of **8** and parent ligand JF$_{635}$-HaloTag ligand (**23**). (**g**–**j**) Fluorescence microscopy images of live HEK293T cells expressing msGFP-HaloTag fusion localized to the mitochondrial outer membrane after incubation with either JF$_{635}$-HaloTag ligand (**23**; **g**,**h**) or biotin-JF$_{646}$-HaloTag ligand (**8**; **i**,**j**) and counterstained with Hoechst 33342. (**k**) Plot of the ratio of JF$_{646}$ or JF$_{635}$ cellular fluorescence intensity to msGFP cellular fluorescence intensity. (**l**,**m**) SDS-PAGE/in-gel fluorescence (**l**) and quantification (**m**) showing the amount of msGFP fusion protein bound to streptavidin

after labeing with ligands **23**, **8**, or **7**. (**n**) Absorbance of **7** or **8** in the absence or presence (+HT) of excess HaloTag protein.

ACKNOWLEDGEMENTS

We thank A. Tebo and A. Waring (Janelia) for purified HaloTag protein. This work was supported by grants from the National Institutes of Health (MH061876 and NS097362 to E.R.C.) and the Howard Hughes Medical Institute. E.R.C. is an investigator of the Howard Hughes Medical Institute. J.D.V. was supported by a postdoctoral fellowship from the National Institutes of Health (F32 NS098604) and the Warren Alpert Distinguished Scholars Fellowship award.

AUTHOR CONTRIBUTIONS

The authors collectively conceived the project. P.K. contributed organic synthesis. J.D.V. contributed cultured cell imaging and biochemical experiments. L.D.L contributed spectroscopy measurements. L.D.L. and E.R.C. directed the project. P.K. and L.D.L. wrote the paper with input from the other authors.

REFERENCES

1. Lavis, L.D. Chemistry is dead. Long live chemistry! *Biochemistry* **56**, 5165-5170 (2017).
2. Los, G.V. et al. HaloTag: a novel protein labeling technology for cell imaging and protein analysis. *ACS Chem Biol* **3**, 373-382 (2008).
3. Keppler, A. et al. A general method for the covalent labeling of fusion proteins with small molecules in vivo. *Nat Biotechnol* **21**, 86-89 (2003).
4. England, C.G., Luo, H. & Cai, W. HaloTag technology: a versatile platform for biomedical applications. *Bioconjug Chem* **26**, 975-986 (2015).
5. Deo, C., Sheu, S.H., Seo, J., Clapham, D.E. & Lavis, L.D. Isomeric tuning yields bright and targetable red Ca(2+) indicators. *J Am Chem Soc* **141**, 13734-13738 (2019).
6. Mertes, N. et al. Fluorescent and bioluminescent calcium indicators with tuneable colors and affinities. *J Am Chem Soc* **144**, 6928-6935 (2022).
7. Deo, C. et al. The HaloTag as a general scaffold for far-red tunable chemigenetic indicators. *Nat Chem Biol* **17**, 718-723 (2021).
8. Wilhelm, J. et al. Kinetic and structural characterization of the self-labeling protein tags HaloTag7, SNAP-tag, and CLIP-tag. *Biochemistry* **60**, 2560-2575 (2021).
9. Grimm, J.B. et al. A general method to fine-tune fluorophores for live-cell and in vivo imaging. *Nat Methods* **14**, 987-994 (2017).
10. Wang, L. et al. A general strategy to develop cell permeable and fluorogenic probes for multicolour nanoscopy. *Nat Chem* **12**, 165-172 (2020).
11. Bucevicius, J., Kostiuk, G., Gerasimaite, R., Gilat, T. & Lukinavicius, G. Enhancing the biocompatibility of rhodamine fluorescent probes by a neighbouring group effect. *Chem Sci* **11**, 7313-7323 (2020).
12. Butkevich, A.N., Bossi, M.L., Lukinavicius, G. & Hell, S.W. Triarylmethane fluorophores resistant to oxidative photobluing. *J Am Chem Soc* **141**, 981-989 (2019).
13. Nemoto, Y. & De Camilli, P. Recruitment of an alternatively spliced form of synaptojanin 2 to mitochondria by the interaction with the PDZ domain of a mitochondrial outer membrane protein. *EMBO J* **18**, 2991-3006 (1999).
14. Vevea, J.D. & Chapman, E.R. Acute disruption of the synaptic vesicle membrane protein synaptotagmin 1 using knockoff in mouse hippocampal neurons. *Elife* **9**, e56469 (2020).
15. Promega (techincal note # 9PIG859). www.promega.com/resources/protocols/product-information-sheets/g/halotag-pegbiotin-ligand-protocol/.
16. Grimm, J.B. et al. A general method to improve fluorophores for live-cell and single-molecule microscopy. *Nat Methods* **12**, 244-250 (2015).
17. Fu, M., Xiao, Y., Qian, X., Zhao, D. & Xu, Y. A design concept of long-wavelength fluorescent analogs of rhodamine dyes: replacement of oxygen with silicon atom. *Chem Commun*, 1780-1782 (2008).
18. Koide, Y., Urano, Y., Hanaoka, K., Terai, T. & Nagano, T. Evolution of group 14 rhodamines as platforms for near-infrared fluorescence probes utilizing photoinduced electron transfer. *ACS Chemical Biology* **6**, 600-608 (2011).
19. Grimm, J.B. et al. A general method to optimize and functionalize red-shifted rhodamine dyes. *Nat Methods* **17**, 815-821 (2020).